SYNTHESIS, CHARACTERIZATION AND CYTOTOXICITY EVALUATION ON ZINC DOPED HYDROXYAPATITE IN COLLAGEN MATRIX

C. L. POPA[a,b], C. M. BARTHA[a,c], M. ALBU[d], R. GUEGAN[e], M. MOTELICA-HEINO[e], M. C. CHIFIRIUC[f], C. BLEOTU[f,g], M. L. BADEA[h], S. ANTOHE[b,i,*]

[a]*National Institute for Materials Physics, P.O. Box MG 07, Magurele, Romania,*
[b]*University of Bucharest, Faculty of Physics, 405 Atomistilor Street, P.O. Box MG1, 077125, Magurele, Romania,*
[c]*Physics Faculty, West University of Timisoara, Bd. V. Parvan 4, 300223 Timisoara, Romania*
[d]*Collagen Department, National Research & Development Institute for Textiles and Leather (INCDTP) – Division, Leather and Footwear Research Institute, Ion Minulescu Str.93, 031215 Bucharest, Romania*
[e]*Institute for Earth Sciences, UMR 7327, CNRS-University of Orléans, 45071 Orléans Cedex 02, France*
[f]*Microbiology Immunology Department, Faculty of Biology, University of Bucharest, 1–3 Portocalelor Lane, Sector 5, 77206 Bucharest, Romania*
[g]*Stefan S Nicolau Institute of Virology, 285 Mihai Bravu, 030304 Bucharest, Romania*
[h]*University of Agronomic Sciences and Veterinary Medicine, 59 Mărăşti Blvd., 011464, Bucharest, Romania*
[i]*Academy of Romanian Scientists, Splaiul Independentei 54, 050094, Bucharest, Romania*

The goal of this study was to obtain at low temperature a functional nano-composite with characteristics similar to the natural bone by using a cost effective method. The structure and morphology of collagen coated zinc doped hydroxyapatite bio-composites (Zn:HAp-CBc) were examined by X-Ray diffraction (XRD) and Scanning Electron Microscopy (SEM). XRD analysis revealed that the unique hexagonal $Ca_{10}(PO_4)_6(OH)_2$ in P_{63m} space group was observed in the obtained nanocomposites Zn:HAp-CBc. The cytotoxicity of the Zn:HAp-CBc was studied on HeLa cell lines. Cell cycle distribution after treatment was examined by flow cytometry analysis. Our preliminary *in vitro* studies revealed that the obtained composites based on Zn doped HAp embedded in collagen matrix have excellent biocompatibility and support their further characterization by *in vivo* approaches and development as a biomaterial used in bone regeneration.

(Received April 24, 2015; Accepted June 12, 2015)

Keywords: Zinc, Hydroxyapatite, Collagen, Bio-composite

1. Introduction

According to a report prepared by the American Association of Orthopaedic Surgeons in 2002, bone is the second most commonly transplanted material, surpassed only by blood transfusion. In order to repair severe bone injuries, caused mainly by congenital deformities, trauma, tumor resection or different degenerative diseases like osteomyelitis [1-2], bone grafts are required. In this context, the difficulty arises when choosing one of the three possible types of grafts. The first possibility is the use of an autograft. This involves harvesting a bone from the patient's body in order to reimplant it. Although it is the most widely used grafting technique, the

*Corresponding author: santohe@solid.fizica.unibuc.ro

amount of tissue that can be used is limited, and the additional surgery that the patient has to endure causes more pain and suffering without forgetting the increased risk of post-surgical infection [3]. Another possibility for bone grafting is the use of an allograft, which involves the harvest of bone tissue from an organ donor. Although this technique is less invasive than the first one, there is a higher risk of an infectious disease being transmitted from the donor to the patient [3]. Therefore, modern medicine has been focused on finding a better solution for the bone grafting problem. In this context, a third approach has emerged in the form of synthetic bone grafts. Thus, researchers worldwide have focused their attention on finding a material that can mimic the human bone tissue.

The human bone is an extracellular matrix composed of two main parts: an inorganic part, where a major component is hydroxyapatite (HAp), with the chemical formula $Ca_{10}(PO_4)_6(OH)_2$, and an organic part consisting of collagen fibrils [4]. In this matrix the collagen fibers are aligned with the *c-axes* of the HAp nanocrystals [5]. Therefore, synthetic hydroxyapatite is a good candidate for bone regeneration due to the biocompatible and osteoconductive properties that it possesses [1]. It has already been used as bone filling or as coating on implanted medical devices such as orthopedic prostheses [1, 6]. In order to enhance certain properties of HAp, such as solubility, bioactivity and osteoinductivity, researchers have tried to include in its structure different ions through ionic substitutions [7-13]. A special attention has been paid to zinc (Zn) as a doping material. Zinc is the most commonly found trace metal in the bone mineral, stimulating bone formation *in vivo* and *in vitro* and inhibiting osteoclastic bone resorption *in vivo* [7,14]. Furthermore, recent studies have demonstrated that the incorporation of Zn into implants speeds the bone formation process around the material [15-17].

Given the fact that synthetic hydroxyapatite can mimic the composition of natural bone, and zinc doped hydroxyapatite enhances the properties that HAp exhibits, in order to create a better biomaterial that could minimize the risk of triggering a defensive response from the host tissue, the structure of the natural bone must also be mimicked. This can be achieved by including in the synthetic composite the characteristics of the organic part of the human bone matrix. 89% of the bone organic matrix is comprised of collagen [3, 18]. Collagen is a natural polymer that can be found in various tissues such as skin and bone (Type I), cartilage (Type II) and blood vessel walls (Type III) [1]. It has been used in tissue engineering and repair due to its outstanding biocompatibility, being easily resorbed by the human body and allowing a good attachment to cells [1,19-22]. Recent studies have proven that collagen and hydroxyapatite devices inhibit the growth of bacterial pathogens, thus minimizing the risk of post-surgical infections occurring after implanting prostheses [1, 23].

The increasing need for new biomaterials with enhanced properties has determined researchers worldwide to try to mimic the characteristics of the natural human tissues. Given the fact that the bone tissue is a complex system, its synthetic replication has to take into account many variables. By combining many composites naturally found in the human hard tissue we hope to create a material that could be integrated in the living human body without triggering any adverse effects, thus improving the quality of life of the patients who had undergone major orthopedic surgeries.

The present study focuses on the synthesis and characterization of novel of zinc doped hydroxyapatite in collagen matrix. The X-Ray diffraction (XRD) and Scanning Electron Microscopy (SEM) were used to investigate the structural and morphological properties of doped hydroxyapatite bio-composite (Zn:HAp-CBc). The cytotoxic effect of Zn:HAp-CBc on HeLa human cancer cell line was also evaluated in this study.

2. Materials and Methods

2.1 Materials

In order to synthesize the zinc doped hydroxyapatite (Zn:HAp), precursors of calcium nitrate [$Ca(NO_3)_2 \cdot 4H_2O$, Aldrich, USA], ammonium hydrogen phosphate ($(NH_4)_2HPO_4$; Wako Pure Chemical Industries Ltd.) and zinc nitrate hexahydrate ($Zn(NO_3)_6.6H_2O$, Alpha Aesare, Germany, 99.99 % purity) were used. Type I fibrillar collagen in gel form (Coll) with a

concentration of 2.11% (w/w) was extracted from calf hide by acid and alkaline treatments as previously described [24]. Glutaraldehyde was purchased from Merck (Germany). Sodium hydroxide and phosphate buffer solution (PBS), pH 7.4 were of analytical grade.

2.2 Zinc doped hydroxyapatite (Zn:HAp) nanoparticles

Controlled amounts of ammonium hydrogen phosphate and zinc nitrate were dissolved in ethanol. After adding distilled water, the solution was stirred vigorously for 24 h at 40 °C. In a separate container, a stoichiometric amount of calcium nitrate was dissolved in ethanol with vigorous stirring for 24 h at 40°C. The Ca-containing solution was added slowly to the P-containing solution, and then aged at room temperature for 72 h and further at 40 °C for 24 h. The composition ratios in the Zn:HAp (x_{Zn}=0.1) sol were adjusted to have [Ca+Zn]/P as 1.67 [25-27]. The obtained Zn:HAp nanopowders were treated at 80 °C for 6 hours.

2.2.1 Collagen coated zinc doped hydroxyapatite bio-composites (Zn:HAp-CBc) preparation

Zinc doped hydroxyapatite was added to collagen gel and Zn:HAp-CBc with the following ratios: 0:1 (collagen reference), 4:1 (Zn:HAp-CBc_4), 1:1 (Zn:HAp-CBc_1) and 1:0 (Zn:HAp reference) were obtained. All the gel composites had the same collagen concentration, 1.2% (reported to dry substance), pH 7.4 and they were cross-linked with 0.5% GA according to the method previously described [28]. After cross-linking process the gel composites were lyophilized using the Christ Model Delta 2–24 LSC freeze-dryer (Germany) and 3D porous composites were obtained.

2.3 Sample characterization

X-ray diffraction measurements have been obtained using a Bruker D8 Advance diffractometer, with nickel filtered CuKα (λ = 1.5418 Å) radiation and a high efficiency one dimensional detector (Lynx Eye type) operated in integration mode. The measurement parameters have been the 2θ range 15°–140°, step of 0.02° and 34 s measuring time per step. Scanning electron microscopy (SEM) has been used to show the morphology of all the samples using a HITACHI S2600N-type microscope equipped with an energy dispersive X-ray attachment (EDAX/2001 device). The secondary device was useful for the identification of the elemental composition. Moreover the Raman spectra have been recorded. Raman spectra were measured with a micro-Raman spectrometer (in Via, Renishaw, Inc.) in a backscattering geometry using a 50 objective lens. An excitation wavelength at 514 nm emitted by an Ar-ion 10 mW monochromatic laser source and a 1800 lines/mm grating were used for the acquisition of the Raman spectra. Beam centering and Raman spectra calibration were performed before each acquisition using a Si standard with a characteristics peak at 520.3 cm^{-1}. Raman analyses were recorded and treated with Wire 3.3 software.

2.4 Cytotoxicity Assay

HeLa cells were used in our experiments. The cells were cultivated in DMEM:F12 (Invitrogen, NY, SUA) supplemented with 10% heat-inactivated bovine serum and penicillin/streptomycin at 37°C with 5% CO_2. The cell morphology was observed by fluorescence microscopy. Briefly, the cells were fixed in 70% ethanol, colored with 5µg/ml propidium iodide and observed with a Leica DFC450 microscope.

The cytotoxicity was established using Trypan blue staining after the treatment with 100µg/ml compound for 24h. Summarily, after the treatment period, cells were harvested from the substrate and 50 µl of each cellular suspension was mixed to a freshly prepared solution of 50 µl Trypan blue (0.05% in distilled water). The mixed suspension was spread onto a microscope slide, covered with a coverslip and observed by microscopic examination. Nonviable cells appear blue-stained. At least 200 cells were counted per treatment.

2.5 Cell cycle distribution

3 x 10^5 cells were plated in each well of 6 well plates and treated for 72 hour with 100 µg/ml material. After the treatment period, cells were taken from the substrate, fixed in 70% cold

ethanol over night at -20^{0}C, washed twice in PBS, and then incubated 15 min, at 37^{0}C, with RNAse A (1 mg/mL), and 1 h with propidium iodide (100 µg/mL). After staining the cells with propidium iodide, the acquisition was done using an Epics Beckman Coulter flow cytometer. Data were analysed using Flow Jo software and expressed as fractions of cells in the different cycle phases.

3. Results and discussions

The X-ray diffraction spectra of Zn:HAp and Zn:HAp-CBc (Zn:HAp-CBc_1 and Zn:HAp-CBc_4) are shown in Fig. 1. All the diffraction peaks of pure hexagonal HAp (ICCD-PDF#9-432) are detected from the patterns obtained for the Zn:HAp and Zn:HAp-CBc (Zn:HAp-CBc_1 and Zn:HAp-CBc_4) samples. Compared to the Zn:HAp nanoparticles, the broadening of the diffraction peaks of Zn:HAp-CBc shows a decrease in intensity which implies a small grain size and low crystallinity [29]. Furthermore, it can be seen that the peak intensities decrease when the ratio collagen/Zn:HAp (Zn:HAp-CBc_1) increases.

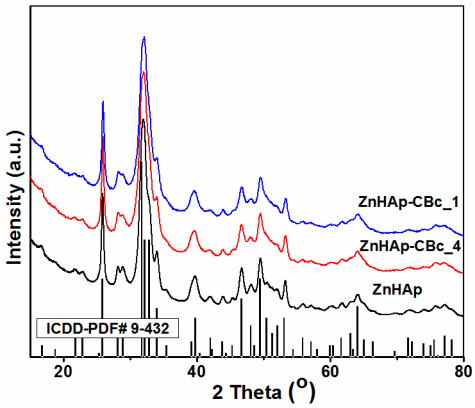

Fig. 1 X-ray diffraction patterns of Zn:HAp, Zn:HAp-CBc_4 and Zn:HAp-CBc_1

In order to investigate the morphology and the porosity of collagen coated zinc doped hydroxyapatite bio-composites (Zn:HAp-CBc), scanning electron microscopy images were recorded. Fig. 2 shows the SEM image of collagen (Fig. 2a), Zn:HAp (Fig. 2b) and Zn:HAp-CBc (Fig. 2c-d). The structure of collagen is presented in Fig. 2a while the ellipsoidal particles at nanometric scale of Zn:HAp were observed in the SEM image Fig. 2b. In Fig. 2c-d can be seen that composite materials have become porous when the ratio Zn:HAp/collagen decreases (Zn:HAp-CBc_1).

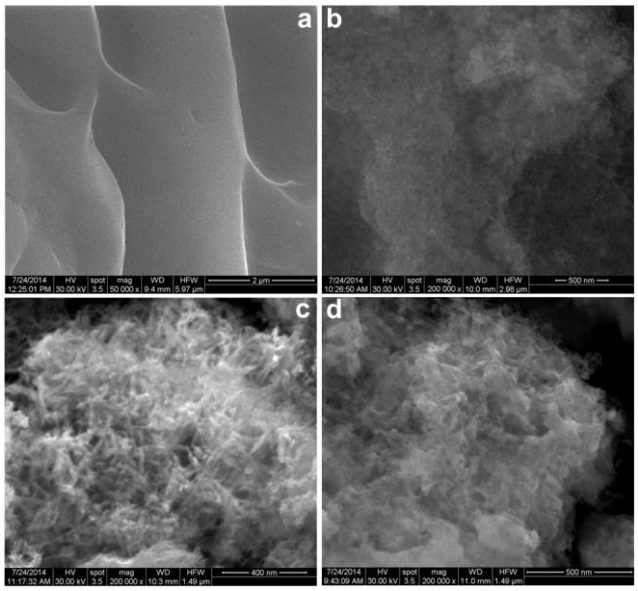

Fig. 2 SEM images of collagen (a), Zn:HAp (b), Zn:HAp-CBc_4 (c), Zn:HAp-CBc_1 (d)

The porosity of composite materials is seen to be directly proportional to the amount of collagen in the samples (Zn:HAp-CBc_1 > Zn:HAp-CBc_4). A good homogeneity was also observed in the samples. Increasing the Zn:HAp content, the ellipsoidal shape of nanocomposite are much visible. The nanoparticles of Zn:HAp are incorporated into a fibrillar network structure of collagen in both samples (Zn:HAp-CBc_1 and Zn:HAp-CBc_4) and the SEM images provide direct evidence. A good homogeneity was also observed in the samples.

The EDX spectrum and mapping of collagen bioceramic material (Zn:HAp-CBc_1) are presented in Fig. 3. EDX spectrum and of Zn:HAp-CBc showed that the main elements present in the sample are calcium, phosphor, zinc, oxygen and carbon. On the other hand, a uniform distribution of constituent elements was observed. These results suggested that Zn:HAp nanoparticles were successfully incorporated in collagen matrix.

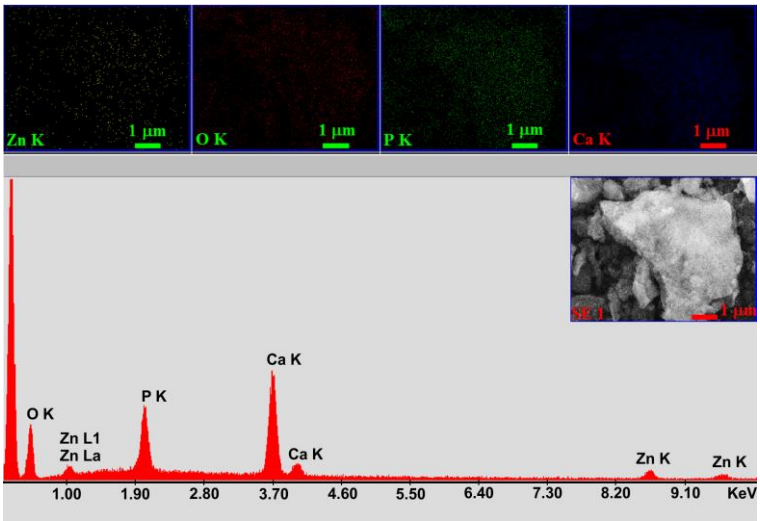

Fig. 3 EDX spectrum and mapping of collagen bioceramic material (Zn:HAp-CBc_1)

The Raman spectra were recorded with a micro-Raman spectrometer (inVia, Renishaw, Inc.) in backscattering geometry. The excitation wavelength used was 514 nm emitted by an Ar-

ion 10 mW monochromatic laser source. The Raman spectra of the Collagen, Zn:HAp (x_{Zn}=0.1), Zn:HAp-CBc_1 and Zn:HAp-CBc_4 are presented in Fig. 4.

In the Raman spectrum of collagen, the most important vibrational bands which are highlighted in Fig. 4 are attributed to: ν amide I (1600-1700 cm^{-1}), ν C-H bending (1400-1500 cm^{-1}), ν amide III (1200-1300 cm^{-1}), ν C-C skeletal (900-1000 cm^{-1}) and ν C-C ring (800-900 cm^{-1}), respectively [30-32]. For the Zn:HAp (x_{Zn}=0.1) sample, the Raman spectrum (Fig. 4) exhibits the main vibrational bands characteristic to the apatite structure. Furthermore, in the spectra recorded for the Zn:HAp-CBc_1 and Zn:HAp-CBc_4 samples, the vibrational bands for the collagen and apatitic structure could be observed. The dominant band (962 cm^{-1}) in the Raman spectra is attributed to the ν_1 PO_4^{3-} internal mode. The other bands are associated with the ν_2 and ν_4 phosphate groups vibrations and are observed at: 430 cm^{-1}, 445 cm^{-1} (ν_2 PO_4^{3-}) and 582 cm^{-1}, 591 cm^{-1}, 607 cm^{-1} (ν_4 PO_4^{3-}).

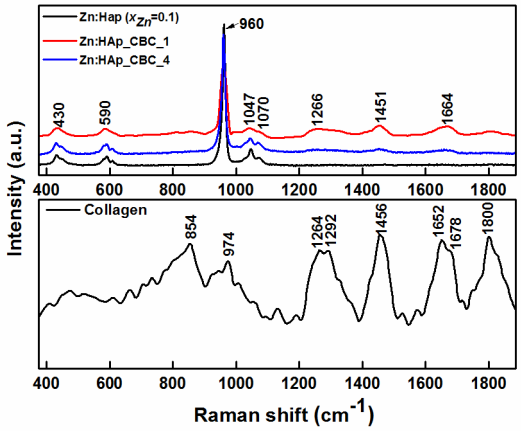

Fig. 4 Raman spectra of the Zn:HAp (x_{Zn}=0.1), Zn:HAp-CBc_1, Zn:HAp-CBc_4 and Collagen

The vibrational band observed at 1047 cm^{-1} is attributed to the ν_3 PO_4^{3-} vibration mode [33, 25]. The assignment of the main bands is summarized in Table 1.

Table 1: Raman bands and their associated vibrational modes.

Wavenumber (cm^{-1})			
Zn:HAp (x_{Zn}=0.1)	Zn:HAp-CBC_1	Zn:HAp-CBC_4	Vibrational modes
432	430	430	ν_2 PO_4^{3-}
445	447	444	ν_2 PO_4^{3-}
582	-	581	ν_4 PO_4^{3-}
591	590	590	ν_4 PO_4^{3-}
607	610	607	ν_4 PO_4^{3-}
962	960	960	ν_1 PO_4^{3-}
1047	1047	1046	ν_3 PO_4^{3-}
-	1070	1072	ν_3 PO_4^{3-}
-	1266	1245	ν Amide III
-	1451	1451	ν C-H bending
-	1664	1664	ν Amide I

The bands associated with the presence of collagen show an increase in intensity, while the bands associated with the apatitic structure show an intensity decrease, becoming wider when the collagen concentration increases.

The TGA and DTA curves behavior of collagen, Zn:HAp-CBc_1, Zn:HAp-CBc_4 and Zn:HAp nanoparticles are illustrated in Fig. 5. The TGA and DTA curves of these samples were performed in the presence of static air at a linear heating rate of 10°C/min from 30°C to 800°C. The TGA curve of Zn:HAp (x_{Zn} = 0.1) does not show a sharp weight loss or a steep slope between 30-800°C. This behavior demonstrates that the decomposition of Zn:HAp does not occur before 800°C. The total weight loss of the Zn:HAp (x_{Zn} = 0.1) nanoparticles is 3.43%. On the one hand, this loss may be associated to the evaporation of adsorbed and structurally incorporated water and removal of residual solvent, on the other hand. According to S. Cameron et al. [34] the adsorbed water was removed from the surface at temperatures greater than 200°C and from pores up to 500°C while the structurally incorporated water was removed at temperatures above 900°C.

The TGA curve of collagen shows one weight loss of 13.7% from 30°C to around 220°C and another two weight losses of 49.13% from 210°C to 490°C and 35.17% from 490°C to 570°C. After 570°C the total weight loss remains constant at 98%. These values are in good agreement with those presented by M. Tegza et al. [35] in previous studies. According to M. Tegza et al. [35] the minimal mass loss in the first range of temperature is due to the dehydration process, while the second mass loss is due to processes of thermal and oxidative destruction characterized by a more rapid decomposition. The third mass loss which occurs in the temperature range from 490°C to 570°C is due to destruction accompanied by burning out of the coke residue.

The influence of collagen is observed in TGA curves of Zn:HAp-CBc_1 and Zn:HAp-CBc_4 nanoparticles. The total mass loss increases when the amount of collagen in the sample is greater (Zn:HAp-CBc_1). The Zn:HAp-CBc_1 nanoparticles showed a mass loss of 9.7 % in the temperature range from 30°C to 287°C, while the mass loss in the temperature range from 287°C to 620°C is about 10%. The total mass loss in the Zn:HAp-CBc_1 nanoparticles was around 20.18% at 620°C. Above 620°C no significant weight loss was observed. When the collagen decreased in the sample (Zn:HAp-CBc_4), the TGA curve shows two marked weight losses. The first mass loss of 7% in the temperature range from 30°C to 270°C. The second weight loss is 5.87% in the temperature range from 270°C to 610°C. Zn:HAp-CBc_4 nanoparticles showed a total weight loss of 12.87% at 610°C. On the other hand, it can be seen that the total weight loss after 620°C remains fairly constant at 12.87%. The thermo-gravimetric analysis (TGA) of the Zn:HAp-CBc showed a decrease in the weight loss with increasing the amount of Zn:HAp nanoparticles (Zn:HAp-CBc_4).

The differential thermal analysis (DTA) curve of the Zn:HAp nanoparticles shows an endothermic peak at around 55°C followed by a broad exothermic peak centered at about 300°C. The endothermic peak below 200°C is due to desorption of adsorbed water and possible elimination of crystal lattice water [36-38]. In agreement with previous studies [39] we can say that the broad exothermic peak centered at 300°C indicates the crystallization of ZnHAp.

In the collagen DTA curve a three stage degradation is observed. The DTA curve of collagen shows significant degradation occurred at 176°C, 330°C and 560°C. According to previous studies [40] the exothermic peak at 176°C is due to loss of water molecules bound to the surface, the exothermic peak at 330°C is due to fragmentation of the macromolecule, while at 560°C the major decomposition occurred due to the formation of gaseous elements. The first endothermic peaks in differential thermal analysis (DTA) curves of the Zn:HAp-CBc_4 and Zn:HAp-CBc_1 at around 60°C and 58°C respectively are considered to be the result of desorption of adsorbed water. The first endothermic peak is followed by an exothermic peak in the DTA curve at 323°C (Zn:HAp-CBc_4) and 327°C (Zn:HAp-CBc_1) indicates the crystallization of Zn:HAp-CBc samples [39].

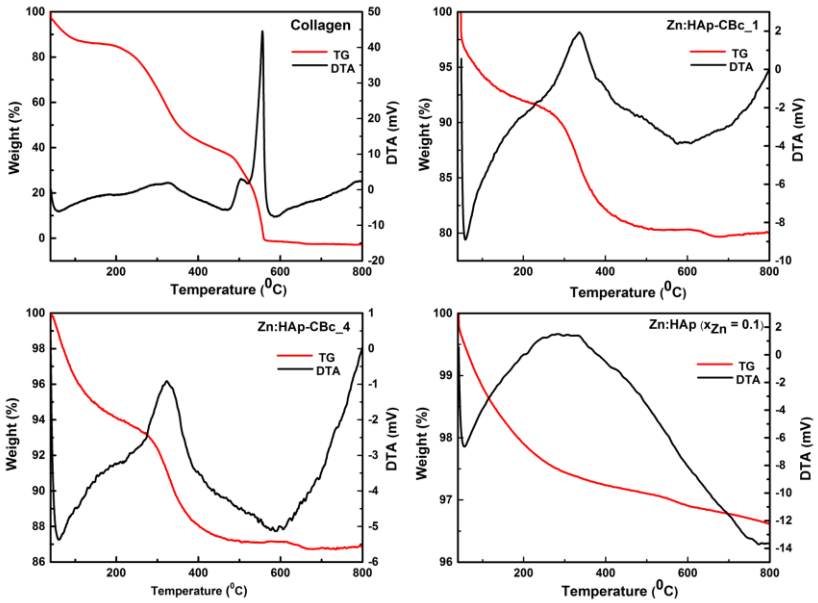

Fig. 5 The TGA and DTA curves behavior of collagen, Zn:HAp-CBc_6, Zn:HAp-CBc_18 and Zn:HAp nanoparticles

Fig. 6 shows that the cells cultivated in the presence of the obtained composites have morphology similar to that of the control, i.e. polygonal cells, homogenously distributed on the surface.

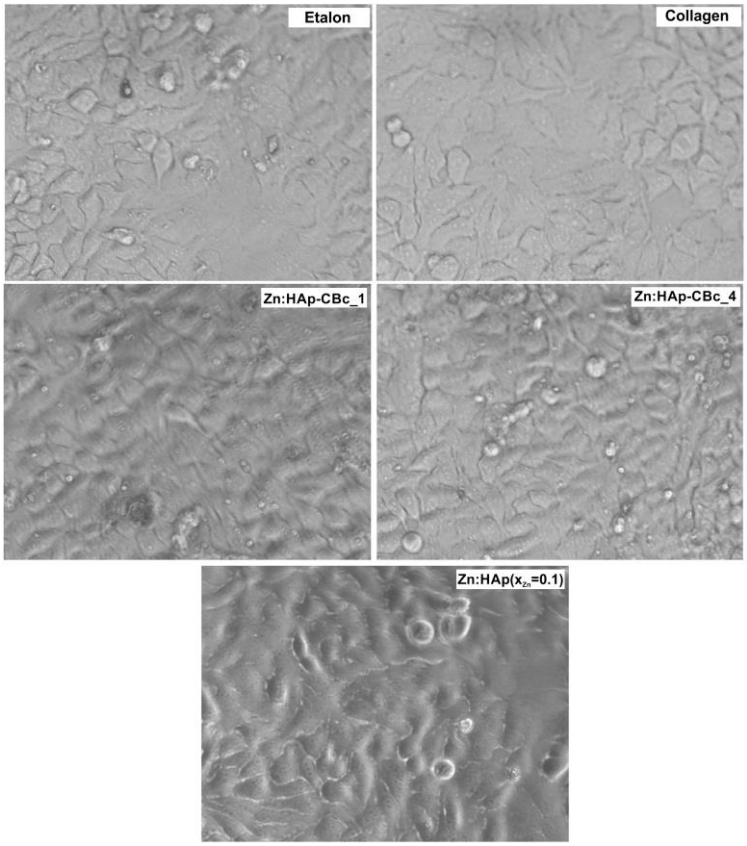

Fig. 6 Morphological studies of HeLa cells (control) following exposure to Collagen, Zn:HAp-CBc_1, Zn:HAp-CBc_4 and Zn:HAp (x_{Zn}=0.1) nanoparticles (10 mg/ml) for 72 h after treatment observed under optic microscopy. Each experiment was performed in triplicate

The influence of the obtained composites on the cellular cycle of HeLa cells was detected further using flow cytometry, with Annexin V-FITC/propidium iodide double-staining of cells. When the HeLa cells were treated with Collagen, Zn:HAp-CBc_1, Zn:HAp-CBc_4 and Zn:HAp no significant changes were found, suggesting that there was no significant difference between the obtained composites and the raw materials with regard to cell proliferation and apoptosis (Fig. 7)

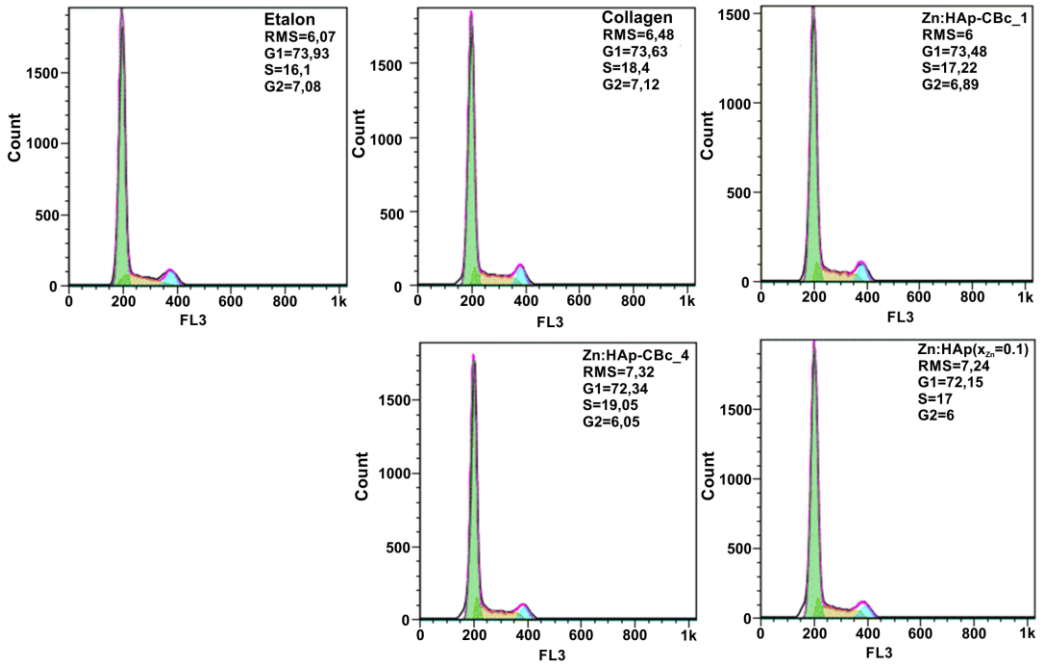

Fig. 7 Cell cycle analysis of HeLa cells cultured with 0.1% DMSO (Control) and treated with Collagen, Zn:HAp-CBc_1, Zn:HAp-CBc_4 and Zn:HAp (x_{Zn}=0.1)

According to previous studies [7, 22-23, 38-43] hydroxyapatite has a high affinity for different species of metal ions. Based on the fact that zinc is the most commonly found trace metal in the mineral phase of the bone, the goal of this work was to study the substitution in the structure of hydroxyapatite coated with collagen of calcium by zinc ions. The results of our studies on cytotoxic effect of Zn:HAp-CBc on HeLa human cancer cell line show a homogenous distribution on the surface with a morphology similar to that of the control (Fig. 6). On the other hand, cell cycle analysis of HeLa cells cultured with 0.1% DMSO (Control) and treated with Collagen, Zn:HAp-CBc_1, Zn:HAp-CBc_4 and Zn:HAp (xZn = 0.1) showed no differences between the obtained composites and the raw materials with regard to cell proliferation and apoptosis (Fig. 7). Moreover, it is very clear that the substitution of calcium by zinc ions in the structure of hydroxyapatite coated with collagen does not affect the general crystal structure (Fig. 1). The results of this study show that the Zn:HAp-CBc samples with controlled particle size can be obtained by co-precipitation method. The collagen and zinc concentrations play an important role in the particle size and the morphology of the particles. EDX analysis (Fig. 3) gives the information regarding the composition of the Zn:HAp-CBc composite materials. It was observed that the constituent elements, C, P, O, Ca and Zn, were uniformly distributed. Additionally, the Raman spectra (Fig. 4) of Zn:HAp-CBc composite materials show the peaks associated to phosphate and carbonate groups and the specific peaks in the region 500-750 cm^{-1} and at 1548 and 1659 cm^{-1} attributed to Amide IV-VII and Amide II, respectively. Based on XRD, SEM, EDAX and *in vitro* results, it was concluded that the Zn:HAp-CBc composite materials could be a viable candidate for future development of bone implants.

4. Conclusions

The present study presents a method for obtaining a novel bio-composite based on zinc doped hydroxyapatite in collagen matrix. The XRD studies have confirmed that hydroxyapatite was formed and the final material was crystallized. Raman investigations of the bio-composite based on zinc doped hydroxyapatite in collagen matrix showed specific absorption bands associated to hydroxyl and phosphate groups characteristic to the hydroxyapatite structure. The mapping studies have evidenced an uniform distribution of the constituent elements.

Our *in vitro* preliminary studies reveal that the obtained composites based on Zn doped HAp embedded in collagen matrix has excellent biocompatibility and support its further characterization by *in vivo* approaches and development as a biomaterial used in bone regeneration.

One of the ultimate goals of engineered biomedicine is to create new materials able to replace damaged natural tissues. The natural hard tissue is a very complex system that has specific properties and functions. In order to replicate this part of the human body, the characteristic of bones must be replicated. Therefore, the synthetic materials used for the reconstruction of bone injuries must mimic the natural components found in the bone tissue. The aim of our research was to study the combination of various synthetic materials in order to improve the quality of the implants. Given the promising results obtained for the Zn:HAp-CBc composite materials, we could say that the novel bio-composite of zinc doped hydroxyapatite in collagen matrix is a cost efficient biomaterial that can be used in biological applications as a bone replacement material.

Acknowledgements

This work was supported by projects IFA-CEA C4-05/2014 and PN II 221/2014. Also this work was supported by the strategic grant POSDRU/159/1.5/S/137750, "Project Doctoral and Postdoctoral programs support for increased competitiveness in Exact Sciences research" cofinanced by the European Social Found within the Sectorial Operational Program Human Resources Development 2007 – 2013.

References

[1] DA Wahl, JT Czernuszka, Eur Cell Mater **11,** 43 (2006).
[2] M Geiger, RH Li, W Friess, Adv Drug Deliv Rev **55,** 613 (2003)
[3] AA Al-Munajjed, NA Plunkett, JP Gleeson, T Weber, C Jungreuthmayer, T Levingstone, J Hammer, FJ O'Brien, J Biomed Mater Res Part B Appl Biomater **90B**(2), 584 (2009)
[4] K Matsunaga, H Murata, T Mizoguch, A Nakahira, Acta Biomater **6**(6), 2289 (2010)
[5] MC Chang, T Ikoma, M Kikuchi, J Tanaka, J Mater Sci Mater Med **13**(10), 993 (2002)
[6] M Vallet-Regi, JM Gonzalez-Calbet, Prog Solid State Chem **32**(1-2):1 (2004)
[7] F Ren, R Xin, X Ge, Y Leng Acta Biomater **5**(8), 3141 (2009)
[8] JC Elliott Structure and chemistry of the apatites and other calcium orthophosphates. Studies in inorganic chemistry, vol. 18. Elsevier, Amsterdam. (1994)
[9] RZ LeGeros, Monographs in oral science, vol. 15. Karger, Basel. (1991)
[10] S Koutsopoulos, J Biomed Mater Res A **62,** 600 (2002).
[11] CS Ciobanu, SL Iconaru, P Le Coustumer, LV Constantin, D Predoi, Nanoscale. Res. Lett. **7**, 324 (2012)
[12] C.S. Ciobanu, C.L. Popa and D. Predoi, J. Nanomater. **2014**, 1 (2014).
[13] C.S. Ciobanu, E. Andronescu and D. Predoi, Dig. J. Nanomater. Bios. **6**, 1239 (2011).
[14] A Ito, M Otsuka, H Kawamura, M Ikeuchi, H Ohgushi, Y Sogo, N Ichinose Curr Appl Phys **5**, 402 (2005)
[15] Y Tang, HF Chappell, MT Dove, RJ Reeder, YJ Lee, Biomaterials **30**(15), 2864. (2009)
[16] A Ito, H Kawamura, M Otsuka, M Ikeuchi, H Ohgushi, K Ishikawa et al, Mater Sci Eng **22**(1), 21 (2002)

[17] A Ito, K Ojima, H Naito, N Ichinose, T Tateishi, J Biomed Mater Res **50**, 178 (2000)
[18] RB Martin, DB Burr, NA Sharkey Skeletal Tissue Mechanics Springer-Verlag, New York. (1998)
[19] D.Predoi, R.A. Vatasescu-Balcan, J. Optoelectron. Adv. Mater. **10**, 152 (2008).
[20] G Voicu, SI Jinga, R Trusca, F Iordache, Dig J Nanomater Bios **9**, 99 (2014)
[21] LC Rusu, DA Kaya, MV Ghica, MG Albu, L Popa, A Butu, CE Dinu-Pirvu, Dig J Nanomater Bios **9**, 317 (2014)
[22] G David, BC Simionescu, S Maier, C Balhui, Dig J Nanomater Bios **6**, 1575 (2011).
[23] GA Carlson, JL Dragoo, B Samimi, DA Bruckner, GW Bernard, M Hedrick, P Benhaim, Biochem Biophys Res Commun **321**(2), 472 (2004)
[24] MG Albu Collagen gels and matrices for biomedical applications Lambert Academic Publishing, Saarbrücken. (2011)
[25] CS Ciobanu, F Massuyeau, LV Constantin, D Predoi Nanoscale Res Lett **6**(1),613. (2011)
[26] CS Ciobanu, SL Iconaru, F Massuyeau, LV Constantin , A Costescu, D Predoi, J Nanomater **2012,** 1 (2012)
[27] C.S. Ciobanu, E. Andronescu, B.S. Vasile, C.M. Valsangiacom, R.V. Ghita and D. Predoi, Optoelectron. Adv. Mater.-Rapid commun **4**, 1515 (2010).
[28] A Lungu , MG Albu , NM Florea , IC Stancu, E Vasile, H Iovu Dig J Nanomater Bios **6**(4), 1867 (2011)
[29] S. Liao, FZ Cui, W Zhang, QL Feng J Biomed Mater Res B **69B**(2), 158 (2004)
[30] JJ Cárcamo, AE Aliaga, R E Clavijo, MR Branes, MM Campos-Vallette Spectrochim Acta Mol Biomol Spectros **86**, 360 (2012)
[31] T Buchwald, M Kozielski, M Szybowicz, Spectrosc-Int J **27**(2), 107 (2012).
[32] J Roman-Lopez, V Correcher, J Garcia-Guinea, T Rivera, IB Lozano, Spectrochim Acta Mol Biomol Spectros **120,** 610 (2014)
[33] CS Ciobanu, SL Iconaru, P Le Coustumer, D Predoi, Vibrational Investigations of Silver-Doped Hydroxyapatite with Antibacterial Properties, J Spectros. (2013)
[34] Cameron S. Chai, Karlis A. Gross, Besim Ben-Nissan, Biomaterials **19**, 2291 (1998)
[35] M Tegza, O Andreyeva, L Maistrenko, Cheminė Technologija **59,** 40 (2012)
[36] K Samar, V Saurabh, Materials Science and Engineering C **30,** 295 (2010)
[37] D. Predoi, Dig. J. Nanomater. Bios. **2**, 169 (2007)
[38] D. Predoi, Dig. J. Nanomater. Bios. **5**, 373 (2010).
[39] K Agrawal, G Singh, D Puri, S Prakash Journal of Minerals & Materials Characterization & Engineering **10,** 727 (2011)
[40] P Falguni, A Basudam, D Santanu Bioresource Technology **101**, 3737 (2010)
[41] SJ Joris, CH Amberg J Phys Chem **75**, 3172 (1971)
[42] C.L. Popa, C.S. Ciobanu, S.L. Iconaru, M. Stan, A. Dinischiotu, C.C. Negrila, M. Motelica-Heino, R. Guegan, D. Predoi, Cent. Eur. J. Chem. **12**, 1032 (2014).
[43] C.S. Ciobanu, F. Massuyeau, E. Andronescu, M.S. Stan, A. Dinischiotu, D. Predoi, Dig. J. Nanomater. Bios. **6**, 1639 (2011).